Molecular Dynamics Study of the Effect of Pressure on an Aqueous NaCl Solution

G. Jancsó* and K. Heinzinger

Max-Planck-Institut für Chemie (Otto-Hahn-Institut), D-6500 Mainz

P. Bopp

Institut für Physikalische Chemie, Technische Hochschule Darmstadt, D-6100 Darmstadt

Molecular dynamics simulations of a 2.2 molal NaCl solution at room temperature and pressure of 1 bar and 10 kbar have been performed employing a modified version of the central-force model of water. The changes in the structural and dynamical properties of the solution resulting from the increase in pressure are reported. The effect of ions on the self-diffusion coefficients of hydration and bulk water and on the IR spectroscopical properties of the solution is also discussed and compared with the available experimental data.

I. Introduction

The study of the effect of pressure on the properties of aqueous electrolyte solutions has not only practical importance but can contribute significantly to our basic understanding of the interactions between ions and their hydration spheres. Molecular Dynamics (MD) investigations of solutions under high pressure allow to observe the effect of density on the motions and interactions of the various molecular species in the solution. The experimental results of high pressure studies of aqueous solutions have extensively been reviewed in recent years [1−3, 3a].

The results of MD simulations of pure water at high pressure with different water models [4−6] agree reasonably with the experimental data and have given substantial information about the structural changes in liquid water resulting from density increase. Thus, and on the basis of the considerable success of the MD simulations of aqueous electrolyte solutions (see e.g. [7]), one can expect that this method can also be successfully applied to describe and predict the effect of increasing pressure (density) on the different properties of aqueous solutions. The only MD simulations in this direction

have been performed on a 0.55 molal aqueous LiI solution with the ST2 model potential for water, at 508 and 308 K under isochoric conditions [8].

In order to study the influence of pressure increase on the structural and dynamical properties of a 2.2 molal aqueous NaCl solution at constant temperature we decided to use the revised central-force potential [9] for water. This potential was found to give a realistic estimate of the shifts of the intramolecular vibrations of the water molecule on condensation and has been also employed in the MD simulations of compressed liquid water [6], of a 1.1 molal $CaCl_2$ solution [10], and of a 13.9 molal LiCl solution [11]. Previous MD simulations of NaCl solutions from this laboratory [12, 13] used the ST2 potential [14] and the latest version of the central-force model developed by Stillinger and Rahman [15]. The structure functions calculated from these MD simulations were in reasonable agreement with each other and with that derived from an X-ray investigation [16]. However, because of the deficiencies in this central-force potential (discussed elsewhere [17]) the predicted internal vibrational frequencies of the water molecules in the hydration spheres and in the bulk water were in error, and in addition the length of the MD simulation of 1.4 ps [13] did not permit the evaluation of dynamical properties (e.g. self-diffusion coefficients).

In the present paper the results of MD simulations of a 2.2 molal NaCl solution at densities corresponding to pressures of about 1 bar and 10 kbar at room temperature are reported. Although a com-

* Permanent address: Central Research Institute for Physics, Hungarian Academy of Sciences, Budapest, Hungary.
Reprint requests to Dr. K. Heinzinger, Max-Planck-Institut für Chemie, Saarstraße 23, P.O. Box 3060, D-6500 Mainz.

parison with the results of other MD simulations at normal pressure and with experimental data will also be made, the main emphasis will be placed on the description and discussion of the changes in the various properties of the NaCl solution due to the increase in pressure. The effect of pressure on the hydration shells of the sodium and chloride ions as obtained from the present MD simulations has been reported elsewhere [18]. First we describe the MD simulations in some detail, then the structural results, and finally the dynamical properties will be discussed.

II. Details of the Simulations

The periodic cube in the simulations contained 200 water molecules, 8 cations and 8 anions. The densities of the solutions at 298 K under 1 bar and 10 kbar are 1.0792 [19] and 1.3067 g cm^{-3} [20], respectively, which leads to periodic lengths of 18.43 and 17.29 Å.

A modified version of the central-force model of water [6, 9] was used; the ion-water and ion-ion potentials were taken from a previous simulation of 2.2 molal NaCl [13] with the exception of the Cl$^-$-water potential. For the latter the potential derived in [21] was employed. The potentials are given in Table 1. For the Coulomb interactions the Ewald summation [22] was used. For the non-coulombic interactions the cut-off distances in units of the periodic length were 0.45, 0.22 and 0.16 for $V_{OO}(r)$,

Table 1. Intermolecular pair potentials employed in the MD simulations. The energies are given in 10^{-12} erg and the distances in Å. For the intramolecular potential of water see [9].

$V_{OO}(r)$ $= 10.04/r + 1858/r^{8.86} - 1.736 \cdot 10^{-2}$
$\cdot \{\exp[-4(r-3.4)^2] + \exp[-1.5(r-4.5)^2]\}$

$V_{OH}(r)$ $= -5.019/r + 0.433/r^{9.2}$
$- 0.694/\{1 + \exp[40(r-1.05)]\}$
$- 0.278/\{1 + \exp[5.493(r-2.2)]\}$

$V_{HH}(r)$ $= 2.509/r + 6.957/\{1 + \exp[29.9(r-1.968)]\}$

$V_{NaO}(r)$ $= -15.22/r - 2.55/r^2 + 8125\exp(-4.526\,r)$

$V_{NaH}(r)$ $= 7.61/r + 0.52/r^2 + 6921\exp(-7.07\,r)$

$V_{ClO}(r)$ $= 15.22/r - 1.849/r^2 + 6304\exp(-3.21\,r)$

$V_{ClH}(r)$ $= -7.61/r + 3.138 \cdot 10^{24}\exp(-34\,r)$

$V_{NaNa}(r)$ $= 23.06/r + 2.375 \cdot 10^{-2}[(2.73/r)^{12} - (2.73/r)^6]$

$V_{NaCl}(r)$ $= -23.06/r + 1.133 \cdot 10^{-2}[(3.87/r)^{12} - (3.87/r)^6]$

$V_{ClCl}(r)$ $= 23.06/r + 476.1/r^6 + 1.523 \cdot 10^4\exp(-3.39r)$

$V_{OH}(r)$ and $V_{HH}(r)$, respectively, and 0.5 for all other potentials.

The starting configuration for the simulations was derived from a previous simulation of an NaCl solution [13]. After a few thousand time steps of equilibration, the simulation comprised 20000 time steps, which is equivalent to a total elapsed time of 5 ps. The total energy showed a small downward trend amounting to about 0.1% over each of the two simulations. The velocities were not rescaled in order to be able to obtain reliable velocity auto-correlation functions. The average temperatures of the simulations were 299 and 303 K for the normal pressure and high pressure runs, respectively. Other technical details of the simulations can be found in [10, 13, 21].

III. Results and Discussion

a) Radial Distribution Functions

The ion-oxygen and ion-hydrogen radial distribution functions (RDF), $g_{xy}(r)$, together with their running integration numbers as defined by

$$n_{xy}(r) = 4\pi\varrho_0 \int_0^r r'^2 g_{xy}(r')\,dr',$$

where ϱ_0 is the number density, are shown in Fig. 1 for the normal pressure (NP) and high pressure (HP) simulations. In the following we will mainly examine the changes in the various RDFs brought about by the pressure increase. The characteristic values of the RDFs are listed in Table 2.

The coordination number of the sodium ion (n_{NaO}) — the value of $n_{NaO}(r)$ at the first minimum of the RDF — is 5.8 and 6.3 for the NP and HP solution, respectively. This increase by about 8% is relatively small compared to the 21% increase in the density of the solutions. If one considers the height of the first peak in g_{NaO} as a measure of the degree of structure around this ion one can conclude that the pressure increase produces a slight decrease in the hydration shell structure. The compression of the solution leads to a broadening of the first peak in $g_{NaH}(r)$ with a 15% increase in $n_{NaH}(r_{m1})$. This increase, compared to the 8% increase in $n_{NaO}(r_{m1})$, shows a penetration of hydrogens belonging to water molecules of the second hydration shell into the region of the first peak in $g_{NaH}(r)$.
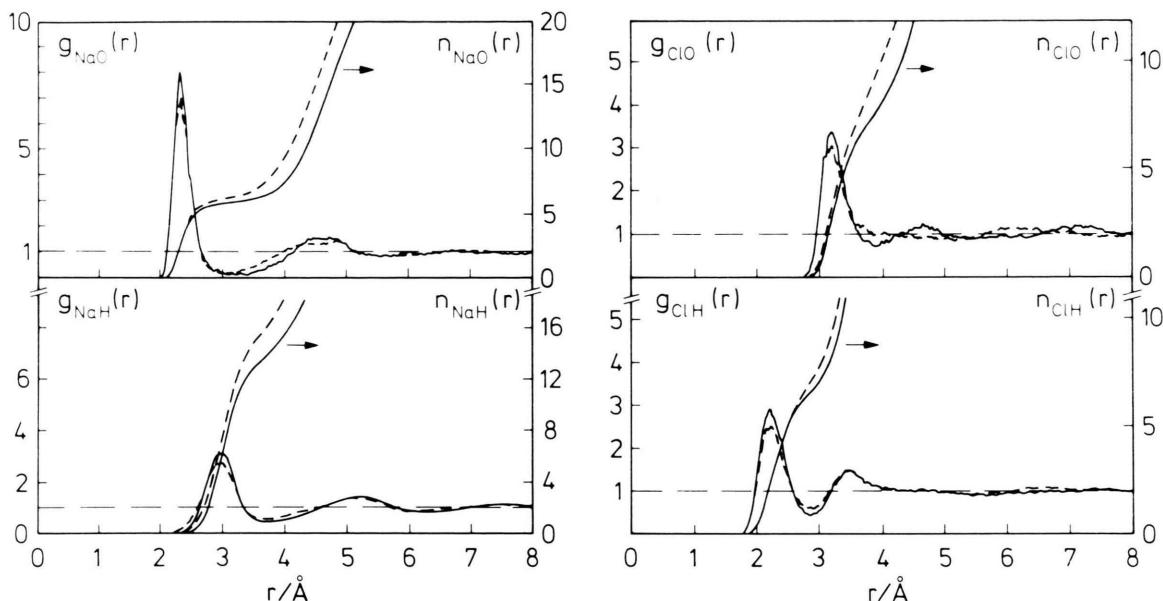
Fig. 1. Ion-oxygen and ion-hydrogen radial distribution functions and running integration numbers for high pressure (HP; dashed line) and normal pressure (NP; solid line) 2.2 molal NaCl. For characteristic values cf. Table 2.

Table 2. Comparison of characteristic values of the radial distribution functions (intermolecular part) for normal pressure (1 bar; denoted by NP) and high pressure (10 kbar; HP) 2.2 molal NaCl solutions. R_i, r_{Mi} and r_{mi} give the distances where $g_{xy}(r)$ equals unity for the i'-th time, has its i-th maximum and minimum, respectively. The distances are given in Å with an uncertainty of at least $\pm$ 0.02 Å. $n_{xy}(r_{m1})$ is the running integration number at the first minimum of $g_{xy}(r)$. $n_{NaO}(r_{m1})$ and $n_{ClO}(r_{m1})$ are considered the coordination numbers of the ions.

x	y		R_1	r_{M1}	$g_{xy}(r_{M1})$	R_2	r_{m1}	$g_{xy}(r_{m1})$	r_{M2}	$g_{xy}(r_{M2})$	$n_{xy}(r_{m1})$
Na	O	NP	2.10	2.30	8.00	2.66	3.10	0.11	4.47	1.58	5.8
		HP	2.10	2.30	7.02	2.63	3.15	0.18	4.8	1.46	6.3
Na	H	NP	2.64	2.95	3.10	3.34	3.70	0.45	5.18	1.42	13.9
		HP	2.59	2.93	2.73	3.32	3.68	0.49	5.05	1.35	16.2
Cl	O	NP	2.95	3.18	3.37	3.60	3.87	0.71	4.62	1.24	7.7
		HP	2.91	3.16	3.10	3.8	–	–	–	–	(9.6)[a]
Cl	H	NP	1.98	2.20	2.93	2.60	2.88	0.45	3.50	1.50	6.7
		HP	1.95	2.15	2.45	2.54	2.85	0.57	3.40	1.50	7.2
O	O	NP	2.65	2.85	2.77	3.20	3.38	0.94	4.53	1.12	4.5
		HP	2.62	2.83	2.81	3.63	4.07	0.75	6.0	1.09	10.8 (6.3)[a]
O	H	NP	1.82	1.93	1.26	2.05	2.50	0.18	3.20	1.53	3.8
		HP	1.90	1.95	1.02	1.97	2.42	0.37	3.15	1.59	4.1
H	H	NP	2.17	2.30	1.54	2.71	3.00	0.78	3.75	1.16	6.3
		HP	2.15	2.25	1.95	2.83	3.08	0.91	3.68	1.11	8.7

[a] This coordination number results if $n_{xy}(r)$ is taken at r_{m1} of the NP case.

The position of the peak maximum in the chloride-oxygen RDF (3.18 Å) is the same as those found in the MD simulations of 1.1 molal MgCl$_2$ [21] and CaCl$_2$ [10], whereas in the previous simulation of 2.2 molal NaCl a value of 3.3 Å was obtained [13]. This difference is due to the improved chloride-water potential [21] employed in the present simulation and those of the MgCl$_2$ and CaCl$_2$ solutions. Neutron diffraction studies of various aqueous solutions show the anionic hydration to be independent of the counterion and yielded a value of 3.20 ± 0.05 Å for the Cl$^-$−O distance in 5.32 molal NaCl [23]. The lack of the counterion effect on the Cl$^-$-hydration, at least as far as the

position of the peak maximum in $g_{ClO}(r)$ is concerned, is confirmed by the MD simulations using the central-force potential.

The height of the first peak in $g_{ClO}(r)$ decreases with increasing pressure similarly to $g_{NaO}(r)$, but contrary to $g_{NaO}(r)$, in the HP solution the second peak in $g_{ClO}(r)$ disappears and the coordination number − taken at the same Cl^-−O-distance ($r = 3.87 \text{ Å}$) − increases by 2 while the increase amounts to only 0.5 for Na^+. This indicates that the hydration shell of Cl^- is softer than that of Na^+ and thus water molecules can more easily be transferred into the first hydration shell by increasing pressure.

From the difference ($\sim 1 \text{ Å}$) in the r_{M1}'s of $g_{ClH}(r)$ and $g_{ClO}(r)$ (see Table 2) it follows that linear hydrogen bonds are preferentially formed with the chloride ions. The increase in the number

Fig. 3. X-ray structure functions for 2.2 molal NaCl from MD simulations at NP (this work) (− · − · −), with the ST2 model for water [12] (− − −), the CF model for water [13] (———), and from an X-ray measurement [16] (· · · · ·). The insertion shows the structure functions at NP (———) and HP (− − −).
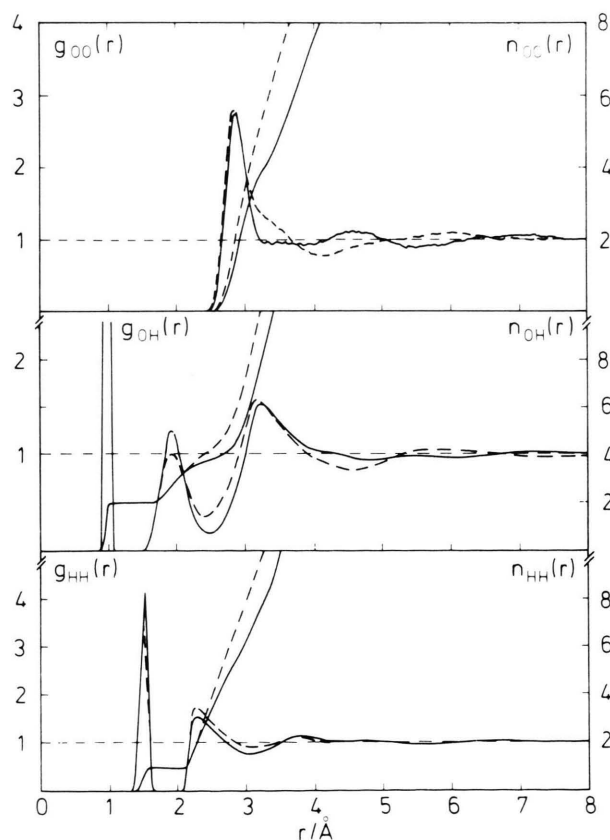

Fig. 2. Oxygen-oxygen, oxygen-hydrogen and hydrogen-hydrogen radial distribution functions and running integration numbers for HP (dashed line) and NP (solid line) 2.2 molal NaCl. For characteristic values cf. Table 2.
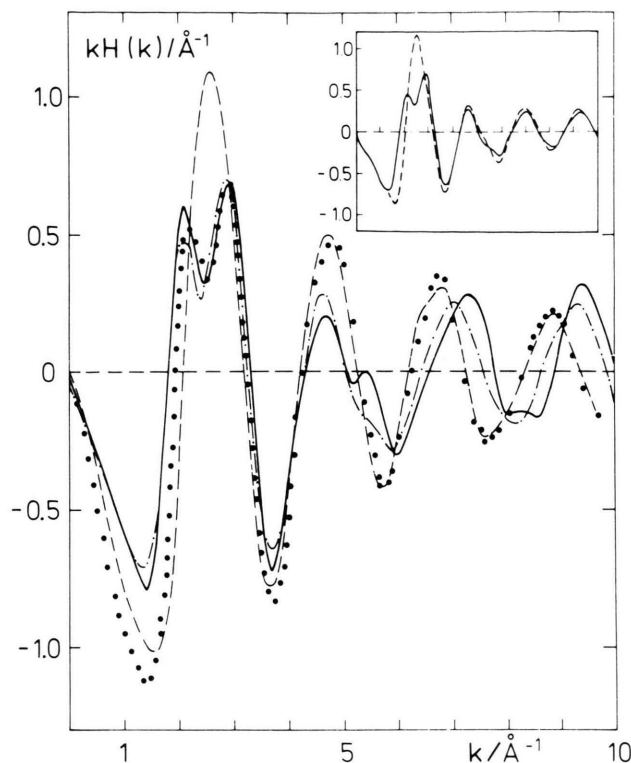
of nearest neighbor hydrogens with pressure is found to be 0.5, just as in the sodium-oxygen case. The changes observed in the Cl^-−O and Cl^-−H RDFs together with those found in the $\cos \Theta$ distributions (vide infra) suggest that the hydration shell structure of Cl^- in the HP solution is less developed than in the NP solution.

In Fig. 2, $g_{OO}(r)$, $g_{OH}(r)$ and $g_{HH}(r)$ and the corresponding $n(r)$ are displayed. Some of the characteristic values of these functions are given in Table 2. From a comparison with the corresponding $g_{OO}(r)$ for pure water (Fig. 3 in [6]) one observes that already in the NP solution the first minimum in $g_{OO}(r)$ is much less pronounced than in pure water. This trend is continued in the HP case. The first peak is wider and the coordination is increased from 4.5 at NP to 6.3 at HP (the integration being carried out to the same distance of 3.38 Å). The changes in $g_{OO}(r)$ as well as in $g_{OH}(r)$ and $g_{HH}(r)$

with pressure are similar to those observed in the MD simulation of pure water [6], however their magnitude is smaller here presumably due to the lower pressure applied (10 kbar instead of 22 kbar). It seems reasonable to conclude that, unlike the first hydration shells of the sodium and chloride ions, the structure of the total solvent water undergoes a significant distortion with increasing pressure.

In Fig. 3 the total X-ray structure function derived from the partial RDFs of the NP solution is compared with those obtained from the MD simulations with the ST2 potential [12], with the central-force potential of Rahman and Stillinger [13], and from experimental X-ray investigations [16]. Both the previous and the present MD simulation with the central-force potential reproduces excellently the experimentally observed characteristic double peak in $kH(k)$ while the MD simulation with the ST2 potential results in a single peak in this region. On the other hand the results of the ST2 simulation are much more consistent with experiment beyond about 5 Å^{-1} than those of the simulations employing the central-force potentials. The humps at around 5.4 and 8.3 Å^{-1} observed in the previous MD simulation [13] have disappeared, which may be ascribed to the modified chloride-water potential. The effect of pressure on the total structure function is shown in the insertion of Fig. 3: The splitting of the main peak disappears and only a single peak is observed at high pressure. No X-ray diffraction study is available for comparison, nevertheless the effect is similar to what is found in pure water [6].

b) Geometry of the Water Molecules

The water model used here allows for internal vibrational motions and can be used with some confidence in predicting the effect of ions and pressure on the average internal geometry.

In the present analysis the water molecules were considered hydration water of Na$^+$ and Cl$^-$ for both NP and HP if their sodium-oxygen and chloride-hydrogen distances were less than 3.10 and 2.86 Å, respectively (approximate positions of the first minima in the $g_{NaO}(r)$ and $g_{ClH}(r)$). The water molecules not belonging to a hydration shell are termed bulk water. The average values of the intramolecular O–H distances (r_{OH}) and HOH angles (α_{HOH}) for the different kinds of water are reported

in Table 3. For water molecules in the hydration shell of Cl$^-$ two values are given, one of them corresponding to the O–H distance involved in hydrogen bonds to the anion and the other one to the second O–H distance.

A comparison of the values for hydration water and bulk water in the NP solution shows, in agreement with the results of previous MD simulations [6, 13, 21], that the presence of ions results in an increase in r_{OH} and in a decrease in α_{HOH}. As could be expected, the chloride ion has a stronger influence on the OH bond directed towards it. The compression of the solution results in an increase by about $6 \cdot 10^{-4}$ Å in the average intramolecular O–H distance (only $2 \cdot 10^{-4}$ Å in the case of the OH bond directed towards the chloride ion) for both the hydration and the bulk water molecules, which is about half of that observed in the MD simulations of pure water ($12 \cdot 10^{-4}$ Å) [6]. Thus in the solution all OH bonds that are not involved in O–H $\cdots$ ion bridges react on pressure in the same way.

It is evident from Table 3 that both the addition of ions to pure water and the increase of the density of the solution by pressure produce a decrease in the average HOH angle, and this together with the changes in the OH bond lengths leads to the increased values of the average dipole moments of water molecules which are also given in Table 3.

Table 3. Average values of the intramolecular O–H distances (r_{OH}), HOH angles (α_{HOH}) and dipole moments (μ) of hydration water and bulk water of NP and HP 2.2 molal NaCl and pure water.

		r_{OH} (Å)	α_{HOH} (degree)	μ (D)
Hydration water	Na$^+$ NP	0.9774	100.32	1.983
	HP	0.9779	99.96	1.992
	Cl$^-$ NP	0.9795 (0.9751)[a]	100.14	1.987
	HP	0.9797 (0.9758)[a]	99.93	1.992
Bulk water	NP	0.9749	100.74	1.969
	HP	0.9755	100.26	1.980
Pure water [6]	NP	0.9755	100.78	1.970
	HP	0.9767	99.82	1.992
Isolated water molecule[b]		0.9572	104.52	1.86

[a] Value for the O–H bond not engaged in hydrogen bonding with the chloride ion.
[b] The water molecule geometry in the improved CF model [9] is taken from [24].

c) Orientation of the Water Molecules in the Hydration Shells

The orientation of the water molecules in the hydration shell of an ion can be characterized by the cosine of the angle between the dipole moment direction of the water molecule and the vector pointing from the oxygen atom towards the center of the ion. In Fig. 4, NP and HP distributions of $\cos(\Theta)$ are shown for the hydration shells of the sodium and chloride ions.

In the case of the hydration shell of Na^+ the $\cos \Theta$ distributions have a maximum at $\cos \Theta = -1$ and the average values of $\cos \Theta$ are found to be -0.793 and -0.741, corresponding to Θ values of $142.5°$ and $137.8°$, in the NP and HP solutions, respectively. This indicates that the water molecules next to a Na^+ tend to point their dipoles away from the Na^+ in agreement with the previous simulation of a 2.2 molal NaCl solution employing the central-force model [13], and that the increase in pressure decreases the orientation of the water molecules in the hydration shell of Na^+. Simulations with the ST2 water model yielded a preferred orientation of a lone pair orbital of the water molecule towards the Na^+ [12].

The $\cos \Theta$ distribution for the water molecules in the hydration shell of Cl^- in the NP solution demonstrates that predominantly linear hydrogen bonds are formed with the anion, in good accord with the conclusion drawn from the observation of $g_{ClH}(r)$ and $g_{ClO}(r)$ and with what is observed experimentally [23]. On pressure increase the value of $\cos \Theta$ changes from 0.595 to 0.498 (i.e. Θ from 53.5° to 60.1°) and the distribution flattens with an extended tail at negative values. This indicates a decrease in the prevalence of forming hydrogen bonds with the chloride ion.

The decrease in the orientation of the water molecules in the first hydration shells of both ions with increasing pressure can also be seen in Fig. 5, which shows the average values of $\cos \Theta$ as functions of the ion-oxygen distance. While only very small differences are found for Na^+, the effect of pressure is quite pronounced for the hydration shell of Cl^-, where the positions of the extrema of $\langle \cos \Theta \rangle$ shift considerably towards smaller ion-oxygen distances. The qualitative differences in the NP and HP $\langle \cos \Theta \rangle$-curve for Cl^- above 3.9 Å correlate with those of the $g_{ClO}(r)$-curves.
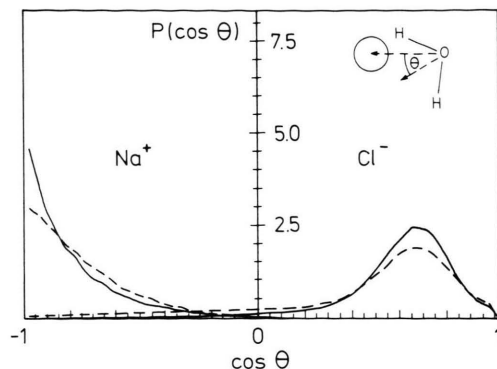

Fig. 4. Distribution of $\cos \Theta$ in the first hydration shells of the ions from MD simulations of 2.2 molal NaCl at NP (solid line) and HP (dashed line). Θ is defined in the insertion.
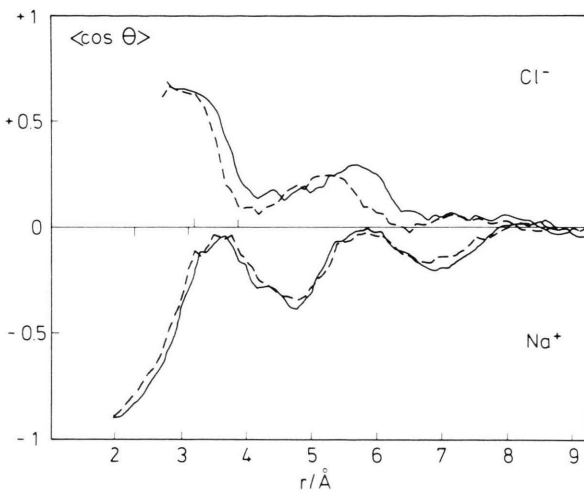

Fi.g. 5. Average values of $\cos \Theta$ as a function of the ion-oxygen distance from MD simulations of 2.2 molal NaCl at NP (solid line) and HP (dashed line). The dashes mark the position of the first maximum and the first minimum in the corresponding RDFs.

For the sake of completeness we should note that the symmetry properties of the hydration spheres are relatively insensitive to the increases in pressure while for the solvent water the changes observed are similar to those found in pure water (for a detailed discussion see [18]).

It is instructive to consider the influence of pressure on the probability of finding a given number of octahedral, hexahedral and tetrahedral directions around Na^+, Cl^- and H_2O, respectively, simultaneously occupied by first shell water molecules. Cones centered at the directions of interest

are defined in the usual way [6, 25], here with an aperture of $40°$, and the configurations are analyzed for simultaneous occupation of the so defined cones by neighboring oxygen atoms. The resulting histograms are displayed in Figure 6.

In the case of Na^+ the probabilities of finding less than six water molecules in the octahedral directions are higher at HP than at NP. The significant decrease in the probability that all the octahedral sites are simultaneously occupied by water molecules may be the consequence of the appearance of a seventh nearest neighor in the hydration sheath of Na^+ in the HP solution. In the case of chloride ions, the rather random distribution of the water molecules in the hydration shell does not change with pressure beyond statistical uncertainties. For the solvent water the changes in the probabilities due to the increase in pressure are smaller than those observed previously for pure water [6], in keeping with the smaller density increase here. We have also calculated the corresponding probability distributions for the bulk water. At normal pressure no difference within the error limits has been found between bulk and pure water. This suggests that the changes observed in $P(n)$ for solvent water with rising pressure results predominantly from the increase in density and that the effect of the presence of ions can be considered as negligible at this concentration.

d) Self-Diffusion Coefficients

The self-diffusion coefficients D have been determined from the velocity autocorrelation functions by means of the Green-Kubo relation

$$D = \lim_{t \to \infty} \frac{1}{3} \int_0^t \langle \boldsymbol{v}(0) \cdot \boldsymbol{v}(t') \rangle \, dt'$$

with

$$\langle \boldsymbol{v}(0) \cdot \boldsymbol{v}(t) \rangle = \frac{1}{N_T N} \sum_{i=1}^{N_T} \sum_{j=1}^{N} \boldsymbol{v}_j(t_i) \cdot \boldsymbol{v}_j(t_i + t),$$

where N denotes the number of particles, N_T the number of time averages and $v_j(t)$ the velocity of particle j at time t.

The correlations have been followed for 0.7 ps, allowing for a sufficient number of time origins t_i in the averaging process.

The normalized velocity autocorrelation functions $\langle \boldsymbol{v}(0) \, \boldsymbol{v}(t) \rangle / \langle \boldsymbol{v}(0)^2 \rangle$ for the ions and oxygens of the NP and HP solutions are shown in Figure 7. As
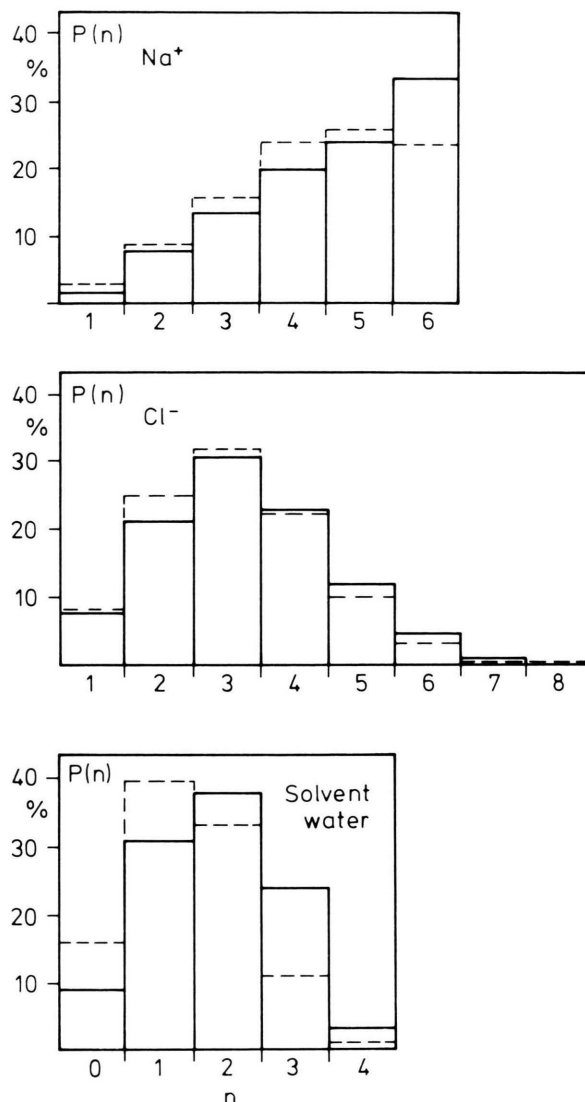

Fig. 6. The probabilities that a given number n of hydration shell water molecules occupy simultaneously octahedral (Na^+), hexahedral (Cl^-) or tetrahedral (water) directions around a central particle at normal pressure (solid) and high pressure (dashed).

was already observed previously [6], the first decay of the correlations is enhanced by the density increase. The effect on the oxygen and Cl^- correlation functions is of similar magnitude while only very small changes are observed in the first decay of the Na^+ correlation. In contrast to this finding, this function displays more structure in the range 0.2−0.4 ps in the HP case than in the NP case.
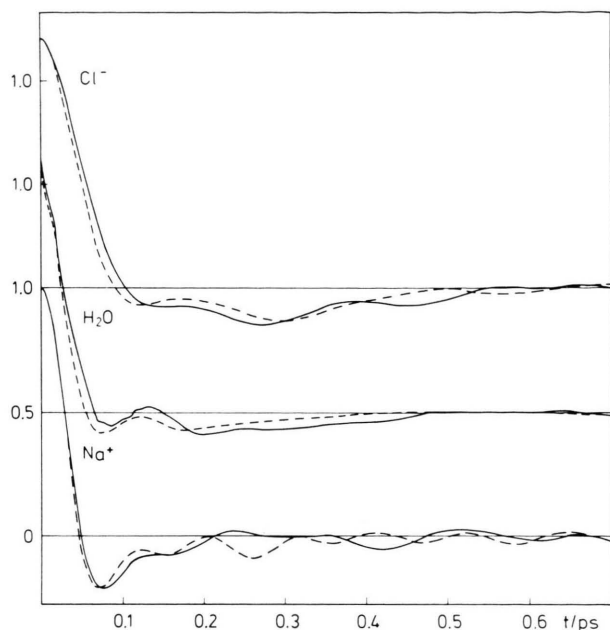
Fig. 7. Normalized velocity autocorrelation functions for Na^+, Cl^- and oxygens from MD simulations at normal pressure (solid line) and high pressure (dashed line).

Table 4. Self-diffusion coefficients of the ions (D_{Na^+}, D_{Cl^-}) and solvent water (D_W) from our MD simulations at normal pressure (NP) and high pressure (HP) and from experiments at room temperature in units of 10^{-5} cm²/s.

		D_W	D_{Na^+}	D_{Cl^-}
MD	NP (299 K)	1.60 (1.83)[a]	0.82	1.08
	HP (303 K)	1.51	0.55	1.25
Exp.	NP (298 K)	1.92 [27]	1.12 [28]	1.60 [28]
			1.30 [29]	1.85 [29]

[a] Extrapolated to 303 K according to [26].

In Table 4 the self-diffusion coefficients calculated from the MD simulations are compiled together with the available experimental data. the self-diffusion coefficient of the solvent water has been corrected for the different temperatures of the NP- and HP-MD simulations by using the temperature dependence of D of pure water [26]. The comparison of the self-diffusion coefficients obtained from the MD simulations with the experimental results shows that the simulation leads to smaller values in all cases. Considering the uncertainties in the experimental results for D_{Na^+} and D_{Cl^-} as indicated by the values reported from different

laboratories, the differences between simulation and experiments seem to be small enough to justify the conclusion that the changes in the self-diffusion coefficients for water and the ions with increasing pressure as calculated from the simulations are reliable − at least qualitatively. Table 4 shows that the 21% density increase is accompanied by about a 20% decrease in the self-diffusion coefficient of solvent water D_W. In pure water at 77 °C a 38% density increase yielded an about 35% decrease in the self-diffusion coefficient [6], which suggests that at high pressures the increased steric hindrances between the molecules plays an important role in controlling the diffusional motion of water molecules both in the pure water and in the solution. In the NP solution D_{Na^+} is found to be significantly smaller than D_{Cl^-}, in good agreement with the experimental results [28, 29]. This can be rationalized as in case of the LiI solution [30] by assuming that the Na^+ is moving through the solution with its hydration shell attached while the Cl^- diffuses essentially without its hydration shell. It is also remarkable that D_{Na^+} decreases while D_{Cl^-} increases with increasing pressure. It is interesting to note that in a recent study of the effect of pressure on the conductance of KCl in heavy water Nakahara et al. [31] found that the residual friction coefficient for K^+ slightly increases with pressure while that for Cl^- decreases.

The self-diffusion coefficients of the water molecules in the three water subsystems − bulk water, hydration water of Na^+ and of Cl^- − have been obtained separately from the velocity autocorrelation functions of the oxygen atoms, which are displayed in Figure 8. It is seen that the effect of the density increase is similar for the three subsystems; essentially a faster decorrelation at short times. The values of the self-diffusion coefficients are listed in Table 5. The values at normal pressure are corrected

Table 5. Self-diffusion coefficients for solvent water (D_W), bulk water (D_{BW}), hydration water of Na^+ (D_{+W}) and of Cl^- (D_{-W}) in units of 10^{-5} cm²/s from MD simulations of a 2.2 molal NaCl solution at normal pressure (NP) and high pressure (HP).

	D_W	D_{BW}	D_{+W}	D_{-W}
NP (299 K)	1.60	1.86	0.90	1.51
	(1.83)[a]	(2.09)[a]	(1.13)[a]	(1.74)[a]
HP (303 K)	1.51	1.76	0.89	1.44

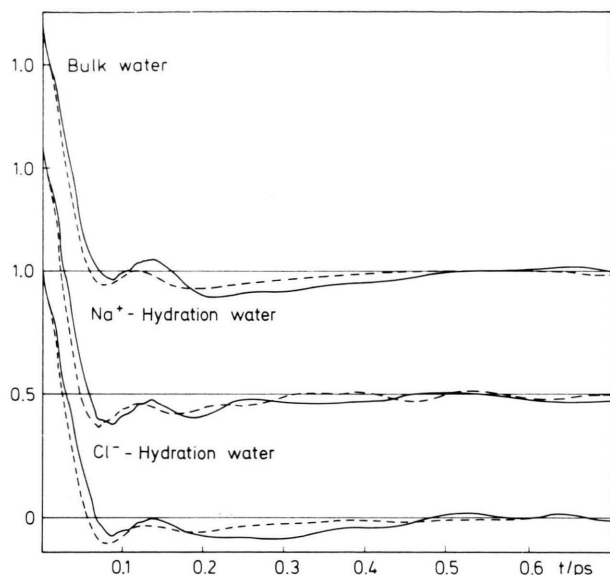[a] Extrapolated to 303 K according to [26].

Fig. 8. Normalized velocity autocorrelation functions of oxygen from MD simulations at normal pressure (solid line) and high pressure (dashed line), calculated separately for bulk water and hydration water of Na^+ and Cl^-.

with the experimentally found temperature dependence for the temperature difference between the two MD simulation runs. The NP results in the solution show that the diffusional motion of the water molecules is reduced in the hydration shells of both ions relative to the bulk water, which is not expected in the case of chloride ion on the basis of its structure-breaking character [32]. This apparently reversed effect may be due to the fact that the properties of a 2.2 molal NaCl solution are far from those of an infinitely dilute solution for which case the considerations concerning the structure-breaking effect of Cl^- strictly apply. A similar effect has already been reported and discussed in detail for the hydration water of the I^- from an MD simulation of a 2.2 molal LiI solution using the ST2 model for water [30]. The increase in pressure seems to slow down the diffusional motion of the water molecules in all of the three water subsystems by about 20%.

e) Hindered Translational and Librational Motions

The spectral densities $f(\omega)$ of the hindered translational motion have been calculated by Fourier transformation from the normalized autocorrelation

functions for the ions (Fig. 7) and separately for the oxygen atoms of the three water subsystems (Figure 8). The results are shown in Figs. 9 and 10.

For the sodium ion $f(\omega)$ in the NP solution (Fig. 9) shows a broad distribution of frequencies in the range $0-400\,cm^{-1}$ with a peak maximum at $120\,cm^{-1}$. As expected, this frequency is much lower than those found for Li^+ (560 and $760\,cm^{-1}$) from an MD simulation of a 2.2 molal LiI solution [30]. The overall shape of $f(\omega)$ for Na^+ is quite similar to that for its hydration water (Fig. 10), from which it can be inferred that the translational motion of the Na^+ is coupled with the translational motion of the water molecules in its first coordination sphere. The pressure rise results in a decrease of the peak at $120\,cm^{-1}$ and in an increase of the spectral density at $310\,cm^{-1}$. Similar changes can be observed in $f(\omega)$ for the hydration water of Na^+; the remarkable increase in the spectral density beyond $270\,cm^{-1}$ indicates that the hindered translational motion of the hydration water molecules becomes more hindered in the HP solution. This is accompanied by an enhancement of the coupling of the translational modes between Na^+ and its hydration water molecules in this region. This result is in
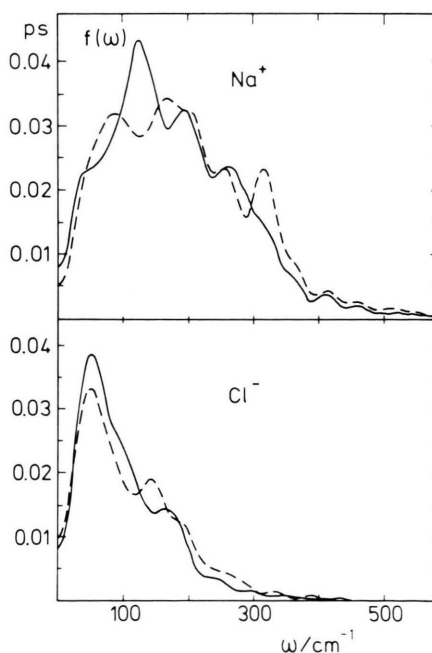

Fig. 9. Spectral densities of the hindered translations of the sodium and chloride ions from MD simulations at normal pressure (solid line) and high pressure (dashed line).
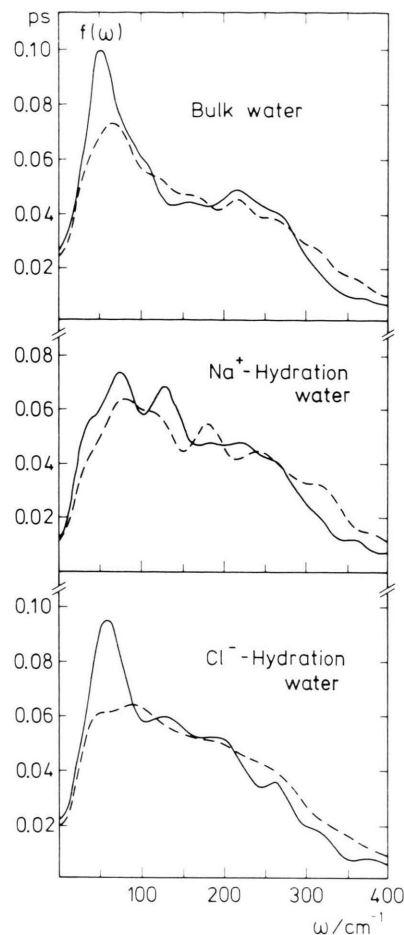
Fig. 10. Spectral densities of the hindered translations of the water molecules from MD simulations at normal pressure (solid line) and high pressure (dashed line), calculated separately for bulk water and hydration water of Na^+ and Cl^-.

harmony with the decrease of the corresponding diffusion coefficients (Tables 4 and 5) with increasing pressure.

The $f(\omega)$ for Cl^- (Fig. 9) shows a main peak at about 50 cm^{-1} with a shoulder in the range $100-200 \text{ cm}^{-1}$. The curve is similar in appearance to that found in an MD study of a 2.2 molal NH_4Cl solution [33] in which the ST2 water model was used. The difference in the spectral densities for Cl^- and for its hydration water (Figs. 9 and 10) are readily apparent and are a consequence of the weaker interactions between the chloride ion and its hydration water as compared to those observed in the case of the sodium ion. The effect of pressure is

more pronounced in the case of the hydration water of Cl^- than in the case of the ion itself. The main peak in the spectral density of the Cl^- motion is remarkably undisturbed by the pressure increase, a shoulder at about 170 cm^{-1} is even shifted to smaller frequencies, in keeping with the higher diffusion coefficient. The chloride hydration water spectrum is not unlike the one for bulk water except for somewhat lower intensities in the region $200-350 \text{ cm}^{-1}$, and the effects of pressure are also quite comparable. The character of the differences in the hindered translation of bulk water in the NP and HP solutions is similar to that found between the NP and HP pure water [6], but the magnitude of the differences (e.g. the decrease in the peak at 50 cm^{-1} corresponding to the $O-O-O$ flexing motion) is smaller here.

The spectral densities of the librations of the water molecules in the NP and HP solutions have been calculated by Fourier transformation from the velocity autocorrelation functions of the hydrogens and are shown in Fig. 11 separately for bulk water and hydration water of Na^+ and Cl^- in the NP solution. The maxima are positioned at 442, 467 and 482 cm^{-1} for bulk water, hydration water of Na^+ and Cl^-, respectively. These values can be compared with those obtained in the previous MD
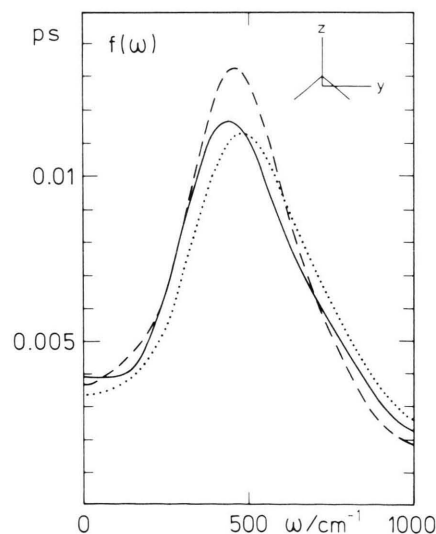

Fig. 11. Spectral densities in the range of the librational frequencies of the water molecules from the MD simulation at normal pressure, calculated separately for bulk water (——) and hydration water of Na^+ (– – –) and Cl^- (·····).

simulation [13]: 437, 477 and 422 cm^{-1}. The only significant difference is in the librational frequencies of the hydration water of Cl$^-$, and this may plausibly be ascribed to the different Cl$^-$-water interaction potentials used in the two MD simulations. It is reasonable to assign the peak maximum around $450-480$ cm^{-1} to librations about the two axes of the water molecule with approximately equal moment of inertia (x and z-axes of the molecule-fixed coordinate system [13] shown in the insertion in Figure 11). The higher librational frequencies of the water moleules belonging to the first coordination spheres of the ions suggest that this particular librational mode becomes more hindered in the hydration shells. In the HP solution the peak maximum are located at 442, 457 and 492 cm^{-1}. The different behaviour of the librations of the hydration water of Na$^+$ and Cl$^-$, as far as the pressure rise is concerned, can qualitatively be explained by the structural changes observed in the NaCl solution with increasing density. While in both cases the pressure increase results in a slight decrease in the structure of the hydration shells of both ions thus favouring a less hindered libration, this is more than compensated in the case of Cl$^-$ by the transfer of second-neighbour water molecules into the immediate neighbourhood of the ion (see g_{ClO} in Figure 1).

f) Intramolecular Vibrations

Velocity autocorrelation functions with a suitable time resolution have been calculated separately for the hydrogens in the three above mentioned water subsystems. The positions of the peak maxima of the spectral densities in the frequency-range of interest are listed in Table 6 together with the corresponding values of pure water. In the NP solution the OH-stretching vibrational frequency in the bulk water has the same value as in pure water while both the sodium and chloride ion cause a shift of about 60 cm^{-1} towards lower wavenumbers. This is in contrast to the widely accepted view according to which the changes in band parameters in aqueous solutions are less sensitive to cations than to anions (see e.g. [34]). A direct comparison with most of the available experimental IR data (see e.g. [35]) is very difficult since the experiments do not give single ion effects on the intramolecular vibrations of water molecules in aqueous electrolyte solutions [10].

Table 6. Frequencies (in cm^{-1}) of the maxima in the spectral densities of the intramolecular vibrations for the various subsystems from the MD simulations of normal pressure (NP) and high pressure (HP) 2.2 molal NaCl solutions.

Mode		Solvent water	Bulk water	Hydration water of		Pure water
				Na$^+$	Cl$^-$	[6]
OH stretching	NP	3510	3537	3472	3467	3533[a]
	HP	3513	3537	3482	3492	3523[b]
HOH bending	NP	1709	1709	1698	1709	1714[a]
	HP	1719	1719	1698	1719	1729[b]

[a] 63 °C; 1 bar. — [b] 77 °C; 22 kbar.

However, in some of the most recent investigations a considerable cation effect has been observed. Kleeberg et al. [36] found in an IR-study of various ternary solutions of monovalent salts large effects on the O–H frequency of water, in keeping with earlier results by Baron et al. [37]. These frequency shifts depend both on the cation present and on the acceptor molecule of the H-bond formed by the water attached to the cation [36]. Zundel [38] who studied the effects of cations on OH-stretching frequencies by IR investigations on poly-anionic films observed a shift of the band maxima corresponding to the OH-stretching vibration of the hydration water molecules towards smaller frequencies. A lowering of the OH-stretching frequency in the presence of cations has also been found by Kuntz and Cheng [39] in their IR studies of water-ion interactions in aprotic solvents. Erikson et al. [40] by using a differential technique to remove the contribution from the bulk water in the IR spectra of aqueous solutions obtained the same band maxima for the OD stretchings of HDO molecules bonded to either Na$^+$ or Cl$^-$. The above experimental data and the results of MD simulations for NaCl, CaCl$_2$ [10] and MgCl$_2$ [41] solutions suggest that the earlier conclusions about the insensitivity of OH-stretching vibrations to cationic effects must be reconsidered

While the OH-stretching vibrations in the bulk water are not influenced by the pressure increase within the accuracy of the present method, a very small shift can be observed in the hydration water of Na$^+$ (Table 6). The only significant change ($+ 25$ cm^{-1}) occurs in the hydration water of Cl$^-$. We note in passing that the spectroscopic correlation between the OH vibrational frequency and the

average O−H distance (the OH-stretching frequency decreases with increasing O−H distance) does not seem to apply for the pressure increase in the solution (Table 3 and 6) in spite of the fact that this correlation was obeyed, at least qualitatively, when the effect of pressure in pure water [6] or the effect of ions [10] were considered. As both the shifts in O−H distance and frequencies are very small in the systems studied here, final conclusions about this point cannot yet be reached.

The only experimental investigation of the effect of pressure on the spectroscopic properties of aqueous NaCl solutions has been carried out by Inoue et al. [42] who have studied the near IR spectra (the band $2v_1 + v_3$) of pure water and of various aqueous solutions from 10 to 55 °C and at pressures up to 5 kbar. For a 3 molal NaCl solution at 25 °C and 4 kbar they observed a shift of 10 cm^{-1} in the band maximum to lower wavenumbers which would correspond to a much smaller change in the fundamental region. The extrapolation of the experimental data (Fig. 9 in [42]) to 10 kbar does not exclude the possibility of the observation of a reversed effect, i.e. the shift of the $2v_1 + v_3$ band to slightly higher frequencies at this high pressure in qualitative agreement with the results of the MD simulations.

The HOH-bending frequencies (v_2) have the same values in the bulk water and hydration water of Cl⁻ while for the hydration water of Na⁺ a smaller value for v_2 was obtained (Table 6). The Na⁺ appears to lower the v_2 frequency of pure water by about 15 cm^{-1}, which compares very favourably with the average value of 24.6 cm^{-1} found for monovalent cations by Falk [43] analyzing literature data on the vibrational spectra of water in solutions and crystalline hydrates. With increasing pressure the positions of the maxima of the peaks corresponding to v_2 have been shifted to higher frequencies by 10 cm^{-1} in the case of bulk water and hydration water of Cl⁻, on the other hand the v_2 frequency of hydration water of Na⁺ has not changed.

IV. Summary and Conclusions

The analysis of the results of our MD simulations of a 2.2 molal NaCl solution at pressures of 1 bar and 10 kbar has shown that the hydration shell structures of Na⁺ and Cl⁻ are slightly distorted upon pressure increase and the H-bonded network of bulk water undergoes a significant distortion. The structural properties of the solution investigated and discussed include among others the radial distribution functions, the internal geometry of water molecules and their orientation in the hydration shells.

Dynamical properties (self-diffusion coefficients, spectral densities) of the solution have been calculated separately for various subsystems such as hydration water of the sodium ion, of the chloride ion, and bulk water. In keeping with recent experimental results [31], the diffusion coefficient of the cation decreases with pressure while that of the anion increases. Single ion effects are usually not readily available experimentally since in most of the cases only the properties of the total water of the solution can be investigated. Therefore, the predictions of the effect of ions and of pressure on the different dynamical properties of the solution appear to be useful and advance our understanding of the properties of aqueous solutions at a molecular level. In those cases where it was possible to compare the results of the MD simulations with experimental data, the agreement was found satisfactory. Furthermore, the applicability and the limits of the potentials presently employed in the MD simulations of aqueous solutions can be tested and directions of their future improvement can be suggested from MD simulations performed at high pressure.

[1] S. D. Haman, in: Chemistry and Geochemistry of Solutions at High Temperatures and Pressures. Phys. Chem. of the Earth Vols. 13 and 14 (D. T. Rickard and F. W. Wickman, eds.), Pergamon Press, Oxford 1981, p. 89.
[2] E. U. Franck, ibid., p. 65.

[3] K. Tödheide, Ber. Bunsenges. Phys. Chem. **86**, 1005 (1982).
[3a] M. Nakahara and J. Osugi, Rev. Phys. Chem. Japan **45**, 69 (1975); ibid. **50**, 66 (1980).
[4] F. H. Stillinger and A. Rahman, J. Chem. Phys. **61**, 4973 (1974).

[5] R. W. Impey, M. L. Klein, and I. R. McDonald, J. Chem. Phys. **74**, 647 (1981).
[6] G. Jancsó, P. Bopp, and K. Heinzinger, Chem. Phys. **85**, 377 (1984); G. Pálinkás, P. Bopp, G. Jancsó, and K. Heinzinger, Z. Naturforsch. **39 a**, 179 (1984).
[7] K. Heinzinger, Physica **131 B**, 196 (1985).
[8] Gy. I. Szász and K. Heinzinger, Earth Planet. Sci.
[9] P. Bopp, G. Jancsó, and K. Heinzinger, Chem. Phys. Letters **98**, 129 (1983).
[10] M. M. Probst, P. Bopp, K. Heinzinger, and B. M. Rode, Chem. Phys. Letters **106**, 317 (1984); M. M. Probst, T. Radnai, K. Heinzinger, P. Bopp, and B. M. Rode, J. Phys. Chem. **89**, 753 (1985).
[11] P. Bopp, I. Okada, H. Ohtaki, and K. Heinzinger, Z. Naturforsch. **40 a**, 116 (1985).
[12] G. Pálinkás, W. O. Riede, and K. Heinzinger, Z. Naturforsch. **32 a**, 1137 (1977).
[13] P. Bopp, W. Dietz, and K. Heinzinger, Z. Naturforsch. **34 a**, 1424 (1979).
[14] F. H. Stillinger and A. Rahman, J. Chem. Phys. **60**, 1545 (1974).
[15] F. H. Stillinger and A. Rahman, J. Chem. Phys. **68**, 666 (1978).
[16] G. Pálinkás, T. Radnai, and F. Hajdu, Z. Naturforsch. **35 a**, 107 (1980).
[17] G. Jancsó and P. Bopp, Z. Naturforsch. **38 a**, 206 (1983).
[18] G. Jancsó, K. Heinzinger, and T. Radnai, Chem. Phys. Letters **110**, 196 (1984).
[19] R. W. Potter and D. L. Brown, Geol. Survey Bulletin 1421-C, U.S. Government Printing Office, Washington D.C. 1977.
[20] L. H. Adams, J. Amer. Chem. Soc. **53**, 3769 (1931).
[21] W. Dietz, W. O. Riede, and K. Heinzinger, Z. Naturforsch. **37 a**, 1038 (1982).
[22] P. P. Ewald, Ann. Physik **64**, 253 (1921).
[23] S. Cummings, J. E. Enderby, G. W. Neilson, J. R. Newsome, R. A. Howe, W. S. Howells, and A. K. Soper, Nature **287**, 714 (1980).
[24] K. Kuchitsu and Y. Morino, Bull. Chem. Soc. Japan **38**, 814 (1965).
[25] G. Pálinkás, T. Radnai, W. Dietz, Gy. I. Szász, and K. Heinzinger, Z. Naturforsch. **37 a**, 1049 (1982).
[26] H. Weingärtner, Z. Phys. Chem. **132**, 129 (1982).
[27] K. Tanaka, J. Chem. Soc. Faraday Trans. I **71**, 1127 (1975).
[28] R. A. Robinson and R. H. Stokes, Electrolyte Solutions, Butterworths, London 1955.
[29] E. Hawlicka, J. Chem. Soc. Faraday Trans. I, in press.
[30] Gy. I. Szász and K. Heinzinger, J. Chem. Phys. **79**, 3467 (1983).
[31] M. Nakahara, M. Zenke, M. Veno, and K. Shimizu, J. Chem. Phys. **83**, 280 (1985).
[32] G. Jancsó, P. Bopp, and K. Heinzinger, KFKI Report 77–101 (1977).
[33] Gy. I. Szász, W. O. Riede, and K. Heinzinger, Z. Naturforsch. **34 a**, 1083 (1979).
[34] B. E. Conway, Ionic Hydration in Chemistry and Biophysics, Studies in Physical and Theoretical Chemistry, Vol. 12, Elsevier, Amsterdam 1981, Chapter 8.
[35] R. E. Verrral, in: Water, A Comprehensive Treatise, Vol. 3 (F. Franks, ed.), Plenum Press, New York 1973, Chapter 5.
[36] H. Kleeberg, G. Heinje, and W. A. P. Luck, private communication.
[37] M. H. Baron and C. de Lozé, J. Chim. Phys. **68**, 1293 (1971); **69**, 1084 (1972); Chem. Phys. Letters **9**, 103 (1971).
[38] G. Zundel, Hydration and Intermolecular Interaction, Academic Press, New York 1969.
[39] I. D. Kuntz, Jr. and C. J. Cheng, J. Amer. Chem. Soc. **97**, 4852 (1975).
[40] A. Eriksson, O. Kristiansson, and J. Lindgren, J. Mol. Structure **114**, 455 (1984).
[41] G. Jancsó, P. Bopp, and K. Heinzinger, to be published.
[42] A. Inoue, K. Kojima, Y. Taniguchi, and K. Suzuki, J. Sol. Chem. **13**, 811 (1984).
[43] M. Falk, Spectrochim. Acta **40 A**, 43 (1984).